Cambridge Centre for Computational Chemical Engineering

University of Cambridge

Department of Chemical Engineering

Preprint ISSN 1473 – 4273

Developing the PAH-PP soot particle model using process informatics and uncertainty propagation.

Markus Sander [1] , Robert I A Patterson [1] , Andreas Braumann [1] , Abhijeet Raj [1] and Markus Kraft [1]

released: 11 January 2010

[1] Department of Chemical Engineering and Biotechnology
University of Cambridge
New Museums Site
Pembroke Street
Cambridge, CB2 3RA
UK
E-mail: mk306@cam.ac.uk

Preprint No. 87

c4e

Key words and phrases: soot, stochastic, particle

Edited by
Cambridge Centre for Computational Chemical Engineering
Department of Chemical Engineering
University of Cambridge
Cambridge CB2 3RA
United Kingdom.

Fax: + 44 (0)1223 334796
E-Mail: c4e@cheng.cam.ac.uk
World Wide Web: http://www.cheng.cam.ac.uk/c4e/

Abstract

In this work we present the new PAH-PP soot model and use a data collaboration approach to determine some of its parameters. The model describes the formation, growth and oxidation of soot in laminar premixed flames. Soot particles are modelled as aggregates containing primary particles, which are built from polycyclic aromatic hydrocarbons (PAH) molecules, the main building blocks of a primary. The connectivity of the primary particles is stored and used to determine the rounding of the soot particles due to surface growth and condensation processes. Two neighbouring primary particles are replaced by one if the coalescence level between the two primary particles reaches a threshold. The model contains, like most of the other models, free parameters that are unknown a priori. The experimental premixed flame data from Zhao et al. [B. Zhao, Z. Yang, Z. Li, M. V. Johnston, and H. Wang. Proc. Combust. Inst., 30(2):1441-1448, 2005] have been used to estimate the smoothing factor of soot particles, the growth factor of PAHs within particles and the soot density using a low discrepancy series method with a subsequent response surface optimisation. The optimised particle size distributions show good agreement with the experimental ones. The importance of a standardised data mining system in order to optimise models is underlined.

Contents

1 Introduction

There is evidence in the literature that polycyclic aromatic hydrocarbons (PAHs) are the precursors of soot molecules [12, 29, 33]. The formation of PAHs and their gasphase chemistry in flames has been investigated in [11, 24, 26, 34]. Electron microscopy studies by Ishiguro et al. [17] and X-ray diffraction experiments by Chen and Dobbins [9] indicate that soot particles are formed by sticking PAHs. Totton et al. [30, 31] support the sticking of PAHs inside a soot particle using a theoretical model involving intermolecular potentials generated from quantum mechanical calculations. Soot particles grow due to surface reactions, condensation of further PAHs, and coagulations with other soot particles [1, 2, 7, 8].

In this work we present a new detailed soot particle model describing soot particles by primary particles that are in turn composed of individual PAHs. This new model is called PAH-PP and is the successor of the ARCS-PP model [8] in which only information of functional sites were contained in the model whereas the PAH-PP model stores the full molecular information. A detailed description of the model will be provided elsewhere. Although the model has an unprecedented level of physical and chemical detail it contains a number of empirical model components which need to be determined from the comparison to experimental data. In this work we fit a smoothing factor s, that describes the smoothing of the surface due to surface growth and condensation, a growth factor g that describes the growth of PAHs within a soot particle and the density of a soot primary particle ρ. These parameters span a multi dimensional parameter space and the question is how to chose parameters bounds, i.e. the interval in which the parameter can lie, that leads to a model prediction that matches the available experiments as close as possible.

One possibility to search for an optimal set of parameters is to generate points in the parameter space uniformly and to evaluate the model at each of these points. This is done most effectively by so called low discrepancy sequences which approximate a uniform distribution in a deterministic fashion but unlike a cartesian grid the speed of convergence is independent off the dimension of the space [3]. Therefore parameter estimations using low discrepancy series require less evaluations of the model then using traditional Monte Carlo methods. Kocis et al. [19] present different possibilities to generate low discrepancy series and investigate their performance. Kucherenko and Sytsko [20] used low discrepancy series in global optimisation problems.

Another possibility to optimise the parameters is to approximate the model by a response surface. Sheen et al. [27] have proposed a technique to estimate the parameters and their errors for a detailed combustion chemistry model using a spectral uncertainty method. This method takes also the propagation of uncertainties into account and estimates confidence intervals for the determined parameters. Braumann et al. [4, 5] have used this method to estimate the parameters in a multivariate population balance model and studied the influence of different objective functions.

Model optimisations and parameter estimations rely on the availability of a large number of experimental data together with their uncertainties. This underlines the importance of a standardized data repository. The PrIMe database [13] stores the data in a standardized XML format and permits to develop new models and optimise them against a large num-

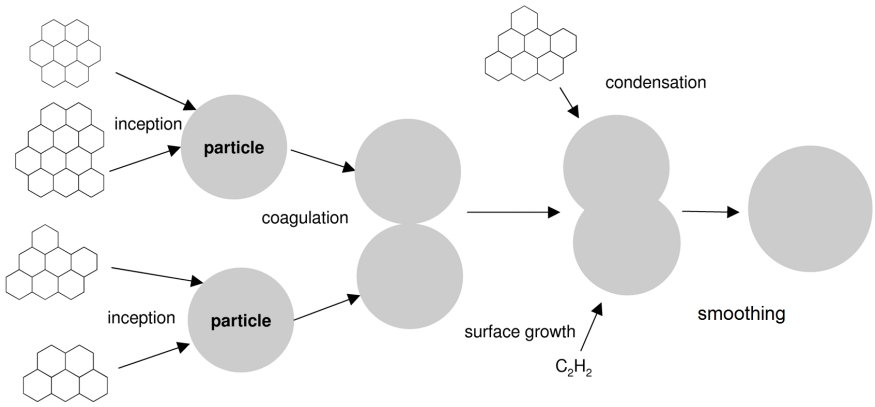

Figure 1: *Processes included in the PAH-PP model.*

ber of experiments. In this paper we shall put experimental data from the literature into PrIMe format and estimate intervals for parameters in the PAH-PP model by an automated procedure which makes use of the PrIMe data models.

2 The PAH-PP Model

The model presented in this work is solved by means of a stochastic algorithm. The algorithm incorporates the evolution of the individual PAHs using a kinetic Monte Carlo algorithm [24, 26], starting from pyrene, present in the gasphase of a sooting flame involving a detailed description of the gasphase flame chemistry. The model considers the growth of the PAH by addition of acetylene via the hydrogen-abstraction carbon-addition (HACA) mechanism [14]. The pyrene production rate along the flame is precalculated using PREMIX [18] including the method of moments to approximate the coupling of the particulate phase and the gasphase. The dimerisation of two PAHs is assumed to incept a soot particle having one primary particle, which contains the two colliding PAHs. The collision of two PAHs does not always create a soot particle, therefore the rate for the dimerisation of PAHs is corrected using a recently determined sticking probability [25]. The growth rate of PAHs within soot particles and therefore not fully accessible to the gasphase is multiplied by a growth factor g, which can vary between 0 and 1. g is one of the free parameters in the model that needs to be determined.

Soot particles can coagulate and forme larger particles. It is assumed that one primary particle p_a of particle P_i and one primary particle p_b of particle P_j are in point contact after the coagulation of particle P_i and P_j. However due to surface growth and condensation processes the soot particles get more spherical. This is incorporated in the model by replacing two neighbouring primary particles by one primary particle. In order to determine this particle rounding, the connectivity of the primary particles within a soot particle is stored as well as the common surface of two neighbouring primary particles. The initial common surface $S(a, b)$ of two neighbouring primary particles p_a and p_b directly after a coagulation event is the sum of the surface of the two individual primary particles. The

common surface $S(a,b)$ of two neighbouring primary particles p_a and p_b changes due to surface growth and condensation processes according to:

$$\Delta S(a,b) = \Delta V(a,b)\frac{s}{R_c} \tag{1}$$

where R_c is the radius of gyration and $\Delta V(a,b)$ the volume change of the primary particles p_a and p_b due to surface growth or condensation. A smoothing factor of s=2 implies that the common surface $S(a,b)$ increases the same area as if the two primary particles would be spherical [22]. A decrease of s leads to a faster rounding of the primary particles. s is the second fit parameter in this work. In order to describe the rounding between two neighbouring primary particles p_a and p_b a coalescence level is defined as

$$C(a,b) = \frac{\frac{S_{sph}(a,b)}{S(a,b)} - 2^{-1/3}}{1 - 2^{-1/3}} \tag{2}$$

where $S_{sph}(a,b)$ is the spherical surface of the two primary particles. Two primary particles are replaced by one primary particle with the same volume if $C(a,b) \geq 1$.

The volume of a particle is calculated as the sum of the volume of the individual primary particles. The surface of the particles incorporates the average coalescence level of the individual primary particles and is approximated by

$$A_{part} = \frac{\sum_{i=1}^{n} A_i}{(C_{avg}(1 - n^{-1/3}) + n^{-1/3})} \tag{3}$$

where n is the number of primary particles, A_i the surface of the i-th primary particle and C_{avg} the average coalescence level of the particle. The inception, coagulation and condensation rate is calculated using the transition regime coagulation kernel K^{tr}, multiplied with the recently determined collision efficiency C_E for PAHs [25]. The transition regime coagulation kernel K^{tr} is the harmonic mean of the slip-flow K^{sf} and free molecular kernel K^{fm} [23]:

$$K^{tr}(A,B) = \frac{K^{sf}(A,B)K^{fm}(A,B)}{K^{sf}(A,B) + K^{fm}(A,B)} \tag{4}$$

where A and B represent particles or PAHs. A and B are particles for a coagulation process, A and B are PAHs for an inception process and A is a particle and B a PAH for a condensation process. The collision diameter of a PAH d_c^{PAH} is

$$d_c^{PAH} = d_A\sqrt{\frac{2n_c}{3}} \tag{5}$$

with $d_A = 1.395\sqrt{3}$Å for a single aromatic ring and n_c the number of carbon atoms in the PAH [15]. A fractal dimension D_f of 1.8 is used to calculate the collision diameter d_c^{part} of a particle [32]:

$$d_c^{part} = \left(\frac{6V}{A}\right)\left(\frac{A^3}{36\pi V^2}\right)^{\frac{1}{D_f}}. \tag{6}$$

The different process included in the model are summarized in Figure 1.

Table 1: *Free parameters in the model*

Name	Variable	Range
Soot density	ρ	$1 \leq \rho \leq 2$
Smoothing factor	s	$0 \leq s \leq 2$
Growth factor	g	$0 \leq g \leq 1$

3 Optimisation

We have selected three free parameters in the PAH-PP model: the soot density ρ, the growth factor of the PAHs in a particle g and the smoothing factor s (Table 1). The soot density has been selected as a free parameter because Totton et al. [30, 31] determined recently 1.12 g/cm^3 as soot density for nascent particles, which is much lower then the usually used soot density of 1.8 g/cm^3 [10, 21].

The parameter vector $\mathbf{x}$ is defined as:

$$\mathbf{x} = (\rho, s, g). \tag{7}$$

The optimisation consists of two consecutive steps: A low discrepancy series method followed by a quadratic response surface optimisation.

In the first step data points in the 3-dimensional parameter space are generated using a Halton [16] low discrepancy series. The model has been evaluated at these points and the objective function

$$\Phi_1(\mathbf{x}) = \sum_{i=1}^{N} (\langle d_i^{exp} \rangle - \langle d_i^{sim} \rangle(\mathbf{x}))^2 \tag{8}$$

determined, where N is the number of experimental data points. $\langle d_i^{exp} \rangle$ is the experimental and $\langle d_i^{sim} \rangle$ is the simulated median of the particle size distribution. The set of parameters $\mathbf{x}^*$ that minimises the objective function Φ_1:

$$\mathbf{x}^* = \underset{\mathbf{x}}{\operatorname{argmin}} \{\Phi_1(\mathbf{x})\} \tag{9}$$

has been determined.

A quadratic response surface optimisation has been performed around the point $\mathbf{x}^*$ to optimise the result further and to estimate the uncertainties in the parameters and in the model response. This methodology has been proposed by Sheen et al. [27] and used by Braumann et al. [6] to optmise a granulation model.

It is convenient to normalise the free parameters $\mathbf{x}$ to $\tilde{\mathbf{x}}$, where $\tilde{x}_k \in [-1, 1], k = 1, 2, 3$. The median of the particle size distribution $\langle d_i^{sim} \rangle(\mathbf{x})$ has been approximated by a second order response surface

$$\langle d_i^{sim} \rangle(\mathbf{x}) \approx \eta(\tilde{\mathbf{x}}) = \beta_0 + \sum_{k=1}^{3} \beta_k \, \tilde{x}_k + \sum_{k=1}^{3} \sum_{l \geq k}^{3} \beta_{kl} \, \tilde{x}_k \, \tilde{x}_l \, . \tag{10}$$

around the point $\mathbf{x}^*$. The coefficients β_0, β_k and β_{kl} have been fitted by evaluating the model at 27 datapoints at $\tilde{\mathbf{x}} = (\tilde{\rho}, \tilde{r}, \tilde{g})$ where $\tilde{\rho}$,$\tilde{r}$,$\tilde{g} \in \{-1, 0, 1\}$. It is assumed that the free parameters $\tilde{\mathbf{x}}$ are Gaussian distributed and have a mean $\tilde{\mathbf{x}}_\mathbf{0}$ and a standard deviation $\mathbf{c}$:

$$\tilde{\mathbf{x}} = \tilde{\mathbf{x}}_\mathbf{0} + \mathbf{c}\,\xi\,, \tag{11}$$

where ξ is normally distributed. The Gaussian distribution of the free parameters influences also the model response. The mean μ can be calculated as [6]:

$$\mu(\tilde{\mathbf{x}}_\mathbf{0}, \mathbf{c}) = \eta(\tilde{\mathbf{x}}_\mathbf{0}) + \sum_{k=1}^{K} \beta_{kk}\, c_k^2\,, \tag{12}$$

Also the variance $\sigma^2(\tilde{\mathbf{x}}_\mathbf{0}, \mathbf{c})$ of the model response can be written in terms of β_0, β_k and β_{kl}. The formula for the variance is beyond the scope of this paper and can be found in [6]. The objective function is based on the principle of moment matching to reduce bias and limit the parametric uncertainties to the experimental error:

$$\Phi_2(\tilde{\mathbf{x}}_\mathbf{0}, \mathbf{c}) = \sum_{i=1}^{N} \left(\left[\langle d_i^{exp} \rangle - \mu_i(\tilde{\mathbf{x}}_\mathbf{0}, \mathbf{c})\right]^2 + \left[\sigma_i^{\exp} - \sigma_i(\tilde{\mathbf{x}}_\mathbf{0}, \mathbf{c})\right]^2 \right)\,. \tag{13}$$

Minimising the objective function using a Matlab routine leads to the optimal set of parameters:

$$(\tilde{\mathbf{x}}_\mathbf{0}^*, \mathbf{c}^*) = \underset{\tilde{\mathbf{x}}_\mathbf{0},\,\mathbf{c}}{\operatorname{argmin}} \left\{\Phi_2(\tilde{\mathbf{x}}_\mathbf{0}, \mathbf{c})\right\}\,. \tag{14}$$

4 Automated model optimisation

```
- <commonProperties>
  - <property description="Inlet pressure of the reactants" label="P" name="pressure" units="atm">
      <value>1</value>
    </property>
  - <property description="Reactant flow rate" label="Fl" name="flow rate" units="g/(cm² s)">
      <value>1.06E-2</value>
    </property>
  - <property description="Maximum flame height above the burner" label="HAB" name="distance" units="cm">
      <value>1.2</value>
    </property>
  - <property name="initial composition">
    - <component>
        <speciesLink preferredKey="C2H4" primeID="s00002578" />
        <amount units="mole fraction">0.242</amount>
      </component>
    - <component>
        <speciesLink preferredKey="O2" primeID="s00010291" />
        <amount units="mole fraction">0.379</amount>
      </component>
    - <component>
        <speciesLink preferredKey="Ar" primeID="s00000048" />
        <amount units="mole fraction">0.379</amount>
      </component>
    </property>
  </commonProperties>
```

Figure 2: *Extract of a PrIMe XML file for a flame.*

The evaluation of the objective function needs fully defined experimental data, ideally with uncertainties. PrIMe XML format stores flame data from premixed laminar sooting

flames in a machine and human readable form. For the purpose of this paper three flames from Zhao et al. [35] have been submitted to the PrIMe data repository in the PrIME format and subsequently used for optimisation. An extract of a PrIMe XML file is shown in Figure 2. This enables a fully automated model optimisation. The PrIMe XML files containing the properties of the flames and the experimental results are used to generate the necessary input files for the software used and to evaluate the objective function. These scripts facilitate the inclusion of a larger number of experimental data than used for this paper. Computational cost of the model evaluation made it necessary to limit our investigation to only three sets of experiments.

5 Results

The model has been optimised against the median of the logarithmic part of the particle size distribution at 5 mm, 8 mm, 10 mm and 12 mm above the burner for the flames A2, A3 and B3 studied by Zhao et al. [35]. This leads to 12 experimental data points. In order to compare our simulation results to the experiments it is necessary to spatially shift the numerical results. This shift is due to effects of probe perturbation during the sampling process. Inserting a probe into a flame changes the gas velocity and cools the flame [28, 29, 35]. A shift of 2.5 mm has been applied for all the flames to account for this effect.

100 low discrepancy series points have been generated and the objective function Φ_1 (Equation (8)) has been evaluated. The minimum of the objective function has been found to be:

$$\mathbf{x}^* = (\rho = 1.63\mathrm{g/cm}^3, s = 1.15, g = 0.23). \tag{15}$$

It has been assumed that the result of the low discrepancy series search has the following uncertainties: σ_ρ=0.2, σ_s=0.2 and σ_g=0.2 and that the experimental error is 0.5 nm for each median data point. Subsequently the response surface optimisation has been performed in the parameter range: $1.43 < \rho < 1.83$, $0.95 < s < 1.35$ and $0.03 < g < 0.43$ to optimise the parameters further and to calculate the uncertainties in the model parameters and model prediction. The minimisation of the objective function Φ_2 (Equation (13)) reveals:

$$\mathbf{x}_\mathbf{0}^* = (\rho = 1.47\mathrm{g/cm}^3, s = 0.98, g = 0.05) \tag{16}$$

and

$$\mathbf{c}^* = (0.17, 0.0, 0.03) \tag{17}$$

The low growth factor g indicates that the PAH in a particle grow much slower then in the gasphase, because they are not fully accessible by the gasphase. The soot density has been found to be between the value determined by Totton et al. [30, 31] and the current literature value.

Figure 3 shows the experimental median, the median before the response surface optimisation (the result of the low discrepancy series optimisation that minimises Φ_1) and the median after the optimisation. The uncertainties of the model response before and after the optimisation are also presented. The response surface optimisation reduces the uncertainties in the parameters and improves the model response for all the three flames.

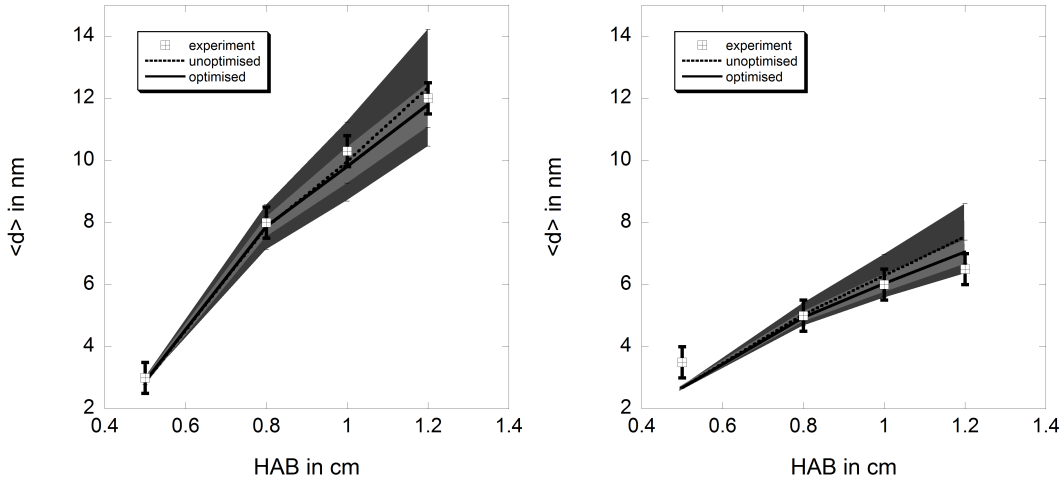

(a) Flame A2

(b) Flame A3

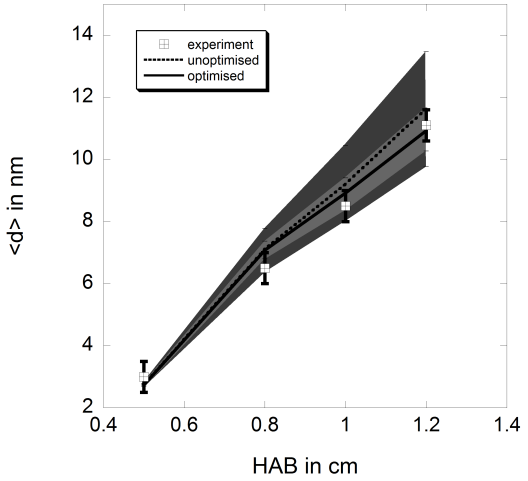

(c) Flame B3

Figure 3: *The experimental median with error bars, the unoptimised median with error (dark grey) and the optimised median with error (light grey).*

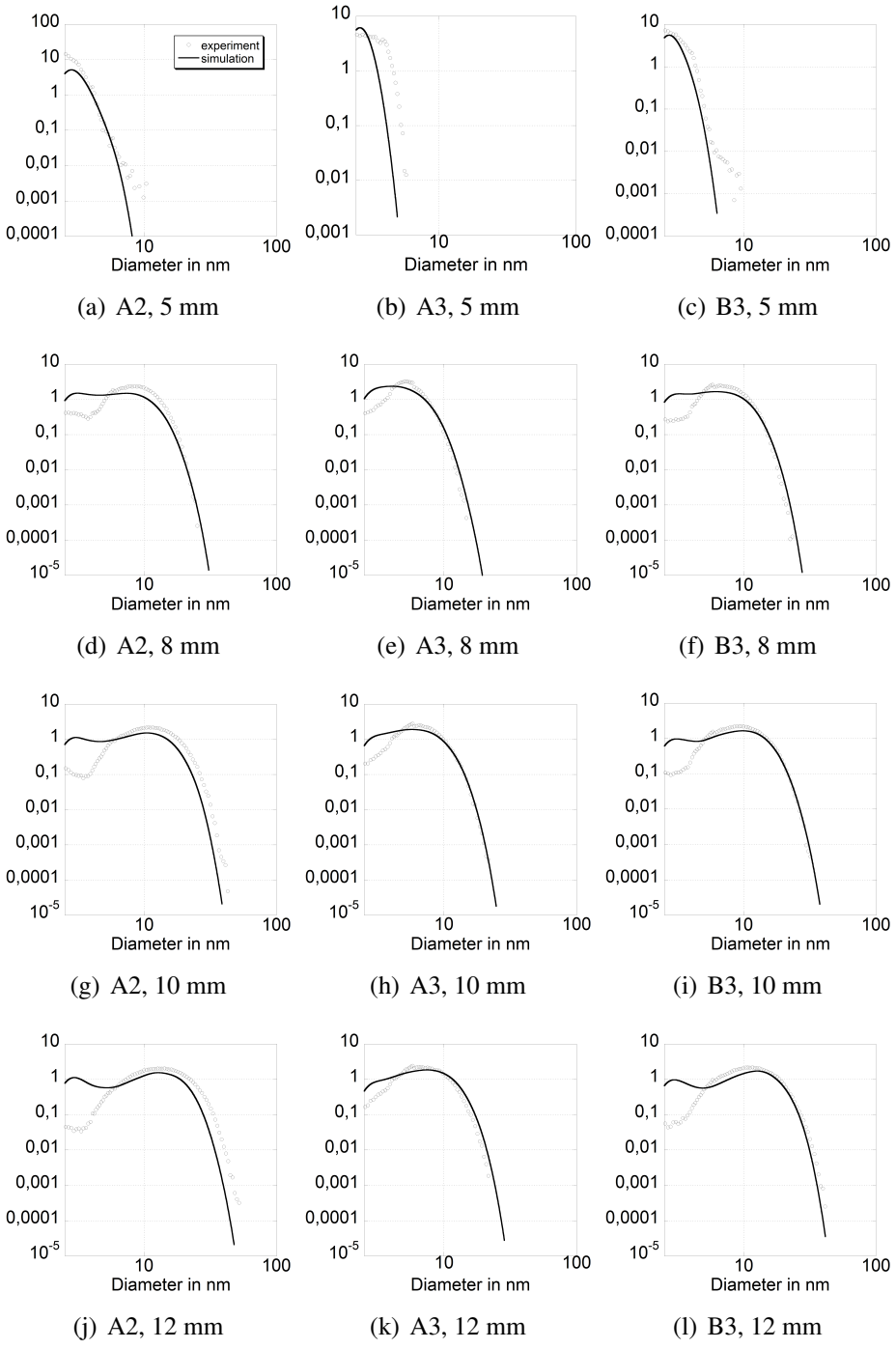

(a) A2, 5 mm (b) A3, 5 mm (c) B3, 5 mm

(d) A2, 8 mm (e) A3, 8 mm (f) B3, 8 mm

(g) A2, 10 mm (h) A3, 10 mm (i) B3, 10 mm

(j) A2, 12 mm (k) A3, 12 mm (l) B3, 12 mm

Figure 4: *Simulated and experimental particle size distribution for the flames A2, A3 and B3 [35] at 5 mm, 8 mm, 10 mm and 12 mm above the burner.*

The model response at 5 mm above the burner is very insensitive to changes in the free parameters because the particles are very small and the properties mainly determined by the gasphase mechanism.

The full particle size distributions are shown in Figure 4. The simulated particle size dis-

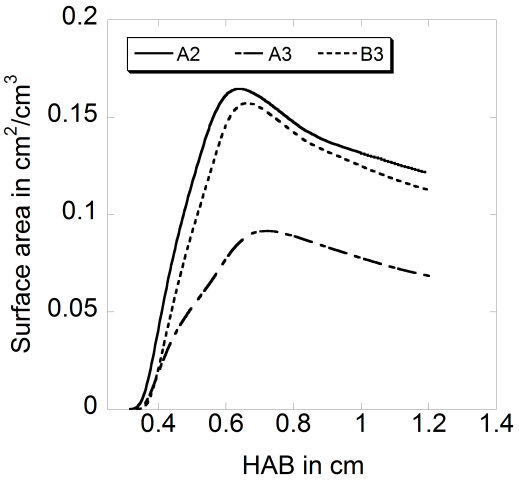

Figure 5: *Surface area of the soot particles.*

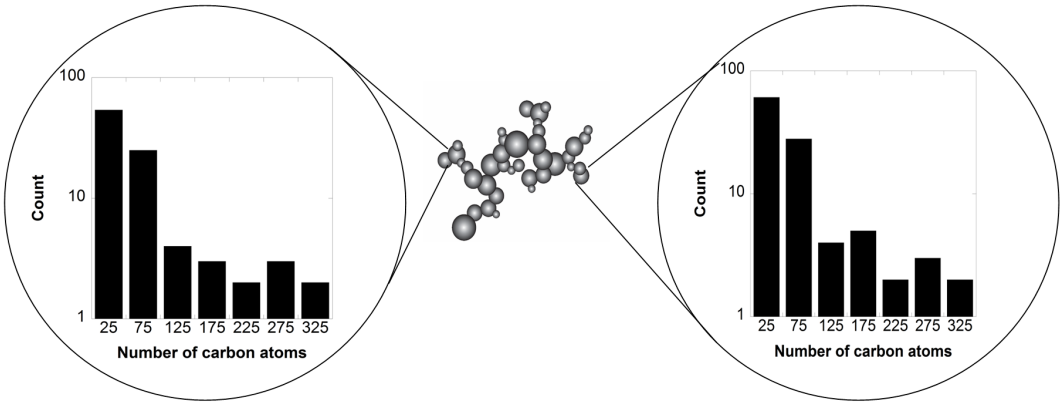

Figure 6: *Histograms of the number of carbon atoms per PAH for one specific primary particle.*

tribution matches the shape of the experiments for the large particles, however the number of small particles is overpredicted. This is not surprising because the model has been optimized specifically to fit the median. Further investigations are necessary to understand these discrepancies.

Figure 5 shows the surface of the soot particles along the flame. The surface of the soot particles increases in the early flame region for all the flames due to a large inception rate and a large number of small soot particles. The coagulation and coalescence of the soot particles in the later flame region reduces the surface of the soot particles.

A simulated TEM image of one of the soot particles together with a typical PAH is presented in Figure 6. Also histograms of the number of carbon atoms per PAH for one specific primary particle is shown.

6 Conclusion

A very detailed soot model that incorporates the composition of each individual primary particle as well as the coalescence of primary particles due to surface growth and condensation events has been optimised against experimental results using a low discrepancy series method followed by a quadratic response surface optimisation. It has been found that PAHs in a soot particle grow much slower then in the gasphase. This could be due to sterical hinderance which prevents the growth species to access the active sites of the PAHs inside a particle. The work also indicates that the current value for soot particle density of 1.8 g/cm^3 is too large and smaller values should be adapted.

The PrIMe data model and a number of scripts have been used to automate model development. An automated model optimisation permits the inclusion of more experimental data in the future. This procedure will facilitate model falsification and hopefully shed some light on the theory of soot particle growth.

Acknowledgements

Financial support from the EPSRC (under grant numbers EP/E01772X/1 and EP/G028672/1) and Churchill College is gratefully acknowledged.

References

[1] J. Appel, H. Bockhorn, and M. Frenklach. Kinetic modeling of soot formation with detailed chemistry and physics: Laminar premixed flames of C_2 hydrocarbons. *Combust. Flame*, 121:122–136, 2000. doi:10.1016/S0010-2180(99)00135-2.

[2] M. Balthasar and M. Kraft. A stochastic approach to solve the particle size distribution function of soot particles in laminar premixed flames. *Combust. Flame*, 133: 289–298, 2003. doi:10.1016/S0010-2180(03)00003-8.

[3] P. Bratley, B. L. Fox, and H. Niederreiter. Implementation and tests of low-discrepancy sequences. *ACM Trans. Model. Comput. Simul.*, 2(3):195–213, 1992. doi:10.1145/146382.146385.

[4] A. Braumann and M. Kraft. Incorporating experimental uncertainties into multivariate granulation modelling. *Chemical Engineering Science*, 65(3):1088–1100, 2010. doi:10.1016/j.ces.2009.09.063.

[5] A. Braumann, M. J. Goodson, M. Kraft, and P. R. Mort. Modelling and validation of granulation with heterogeneous binder dispersion and chemical reaction. *Chem. Eng. Sci.*, 62:4717–4728, 2007. doi:10.1016/j.ces.2007.05.028.

[6] A. Braumann, P. L. W. Man, and M. Kraft. Statistical approximation of the inverse problem in multivariate population balance modeling. *Ind. Eng. Chem. Res.*, 49: 428–438, 2010. doi:10.1021/ie901230u.

[7] M. S. Celnik, R. I. A. Patterson, M. Kraft, and W. Wagner. Coupling a stochastic soot population balance to gas-phase chemistry using operator splitting. *Combust. Flame*, 148(3):158–176, 2007. doi:10.1016/j.combustflame.2006.10.007.

[8] M. S. Celnik, A. Raj, R. H. West, R. I. A. Patterson, and M. Kraft. Aromatic site description of soot particles. *Combust. Flame*, 155:161–180, 2008. doi:10.1016/j.combustflame.2008.04.011.

[9] H. X. Chen and R. A. Dobbins. Crystallogenesis of particles formed in hydrocarbon combustion. *Combust. Sci. Technol.*, 159:109–128, 2000. doi:10.1080/00102200008935779.

[10] M. Y. Choi, G. W. Mulholland, A. Hamins, and T. Kashiwagi. Comparisons of the soot volume fraction using gravimetric and light extinction techniques. *Combust. Flame*, 102:161–169, 1995. doi:10.1016/0010-2180(94)00282-W.

[11] A. D'Anna and J. H. Kent. Modeling of particulate carbon and species formation in coflowing diffusion flames of ethylene. *Combust. Flame*, 144(1-2):249–260, 2006. doi:10.1016/j.combustflame.2005.07.011.

[12] M. Frenklach. Method of moments with interpolative closure. *Chem. Eng. Sci*, 57: 2229–2239, 2002. doi:10.1016/S0009-2509(02)00113-6.

[13] M. Frenklach. Transforming data into knowledgeprocess Informatics for combustion chemistry. *Proc. Combust. Inst.*, 31:125–140, 2007. doi:10.1016/j.proci.2006.08.121.

[14] M. Frenklach and H. Wang. Detailed modeling of soot particle nucleation and growth. *Proc. Combust. Inst.*, 23:1559–1566, 1991. doi:10.1016/S0082-0784(06)80426-1.

[15] M. Frenklach and H. Wang. *Detailed Mechanism and Modelling of Soot Particle Formation*, volume 59 of *Series in Chemical Physics*, pages 162–190. Springer Verlag, Berlin, 1994.

[16] J. H. Halton. On the efficiency of certain quasi-random sequences of points in evaluating multi-dimensional integrals. *Numerische Mathematik*, 2:84–90, 1960. doi:10.1007/BF01386213.

[17] T. Ishiguro, Y. Takatori, and K. Akihama. Microstructure of diesel soot particles probed by electron microscopy: First observation of inner core and outer shell. *Combust. Flame*, 108:231–234, 1997. doi:10.1016/S0010-2180(96)00206-4.

[18] J. Kee, K. Grcar, M. D. Smooke, and J. A. Miller. Premix: A fortran program for modelling steady laminar one-dimensional premixed flames. Technical report, SANDIA National Laboratories, 1985.

[19] L. Kocis and W. J. Whiten. Computational investigations of low-discrepancy sequences. *ACM Trans. Math. Softw.*, 23(2):266–294, 1997. ISSN 0098-3500. doi:10.1145/264029.264064.

[20] S. Kucherenko and Y. Sytsko. Application of deterministic low-discrepancy sequences in global optimization. *Computational Optimization and Applications*, 30: 297–318, 2005. doi:10.1007/s10589-005-4615-1.

[21] C. Park and J. P. Appleton. Shock-tube measurements of soot oxidation rates. *Combust. Flame*, 20:369–379, 1973. doi:10.1016/0010-2180(94)00282-W.

[22] R. I. A. Patterson and M. Kraft. Models for the aggregate structure of soot particles. *Combust. Flame*, 151:160–172, 2007. doi:10.1016/j.combustflame.2007.04.012.

[23] S. E. Pratsinis. Simultaneous nucleation, condensation, and coagulation in aerosol reactors. *J. Colloid Interface Sci.*, 124:416–428, 1988. doi:10.1016/0021-9797(88)90180-4.

[24] A. Raj, M. Celnik, R. Shirley, M. Sander, R. Patterson, R. West, and M. Kraft. A statistical approach to develop a detailed soot growth model using PAH characteristics. *Combust. Flame*, 156:896–913, 2009. doi:10.1016/j.combustflame.2009.01.005.

[25] A. Raj, M. Sander, V. Janardhanan, and M. Kraft. A study on the coagulation of polycyclic aromatic hydrocarbon clusters to determine their collision efficiency. *Combust. Flame*, In Press, 2009. doi:10.1016/j.combustflame.2009.10.003.

[26] M. Sander, A. Raj, O. Inderwildi, M. Kraft, S. Kureti, and H. Bockhorn. The simultaneous reduction of nitric oxide and soot in emissions from diesel engines. *Carbon*, (47):866–875, 2009. doi:10.1016/j.carbon.2008.11.043.

[27] D. A. Sheen, X. You, H. Wang, and T. Løvås. Spectral uncertainty quantification, propagation and optimization of a detailed kinetic model for ethylene combustion. *Proc. Combust. Inst.*, 32(1):535–542, 2009. doi:10.1016/j.proci.2008.05.042.

[28] J. Singh, M. Balthasar, M. Kraft, and W. Wagner. Stochastic modelling of soot particle size and age distribution in laminar premixed flames. *Proc. Combust. Inst.*, 30:1457–1465, 2005.

[29] J. Singh, R. I. A. Patterson, M. Kraft, and H. Wang. Numerical simulation and sensitivity analysis of detailed soot particle size distribution in laminar premixed ethylene flames. *Combust. Flame*, 145:117–127, 2006. doi:10.1016/j.combustflame.2005.11.003.

[30] T. Totton, D. Chakrabarti, A. Misquitta, M. Sander, D. Wales, and M. Kraft. Modelling the internal structure of nascent soot particles. *Combust. Flame*, In Press, 2009. doi:10.1016/j.combustflame.2009.11.013.

[31] T. Totton, A. Misquitta, and M. Kraft. A first principles development of a general anisotropic potential for polycyclic aromatic hydrocarbons. Technical Report 81, c4e Preprint-Series, Cambridge, 2009. URL `http://como.cheng.cam.ac.uk`.

[32] S. Tsantilis and S. E. Pratsinis. Soft- and hard-agglomerate aerosols made at high temperatures. *Langmuir*, 20(14):5933–5939, 2004.

[33] R. L. Vander Wal, A. Yezerets, N. W. Currier, D. H. Kim, and C. M. Wang. HRTEM Study of diesel soot collected from diesel particulate filters. *Carbon*, 45:70–77, 2007. doi:10.1016/j.carbon.2006.08.005.

[34] H. Wang and M. Frenklach. A detailed kinetic modeling study of aromatic formation in laminar premixed acetylene and ethylene flames. *Combust. Flame*, 110:173–221, 1997. doi:10.1016/S0010-2180(97)00068-0.

[35] B. Zhao, Z. Yang, Z. Li, M. V. Johnston, and H. Wang. Particle size distribution function of incipient soot in laminar premixed ethylene flames: effect of flame temperature. *Proc. Combust. Inst.*, 30(2):1441–1448, 2005.